Transient transfection of lung and airway epithelium with gamma interferon as an host directed therapy against tuberculosis

During my PhD, I prepared a dry powder for inhalation (DPI) containing DNA constructs polyplexed with *poly*(ethyleneamine) (PEI). DNA incorporated in the particles remained intact during processing (Figure 1).

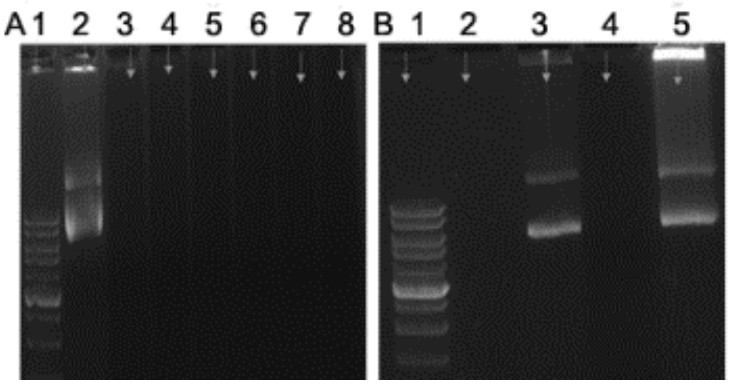

Figure 1: *Gel electrophoresis (A): N/P ratio of 1:2 (PEI to DNA) is sufficient sufficient to ensure that DNA in polyplexes formulated to generate DPI powder by spray drying does not migrate electrophoretically under conditions that induce migration of free plasmid DNA.(Lane 1: 1 Kb DNA ladder, Lane 2: plasmid DNA, Lane 3-8: polyplex at N/P ratios of 1:2, 5, 8, 10, 15 and 20). (B): DNA retains structural integrity after spray-drying. Lane 1: 1 Kb DNA ladder, Lane 2: DNA-polymer polyplex, Lane 3: plasmid DNA, Lane 4: DNA in spray dried powder does not leave the well, Lane 5: DNA is released from spray-dried particles by heparin.*

DPI were engineered to have suitable properties for deep lung deposition, as established by electron microscopy, micromeretics, and cascade impaction, as shown in Figure 3. The median Martin's diameter of the DPI particles by electron microscopy was 1.2μm and the mass median aerodynamic diameter (MMAD) was 2.85μm ±1.8 μm GSD.

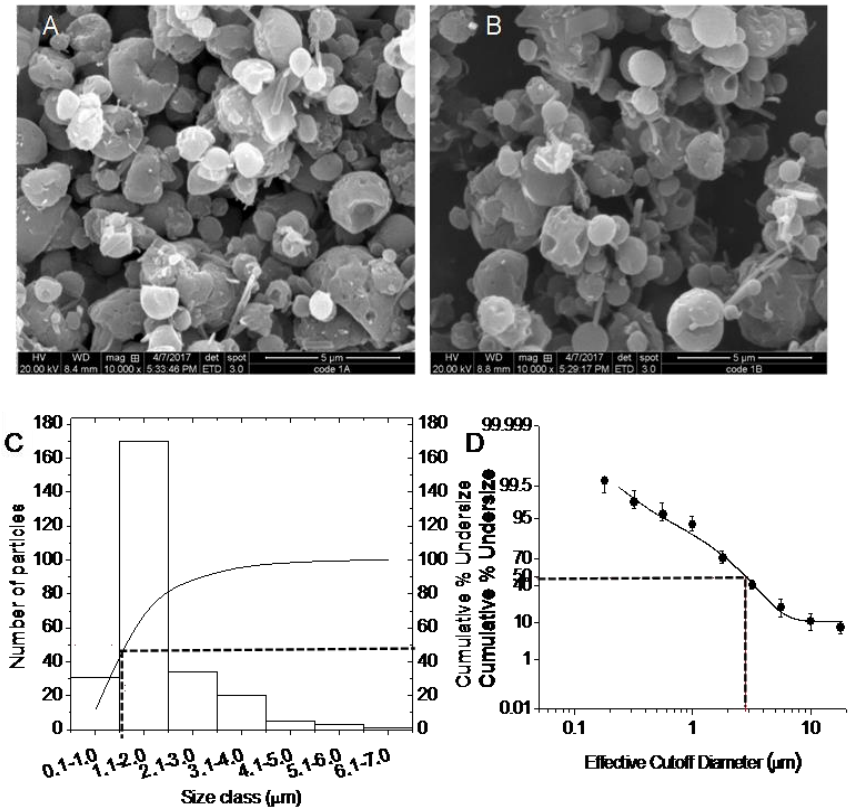

Figure 2 (A, B): Scanning electron micrographs of representative particles from two batches of the spray dried particles at 10,000 × magnification. (C): Histogram of particle size distribution of 264 particles from these two fields, and estimate of median diameter (dotted lines) when cumulative % undersize was plotted against diameter (solid curve).(D): MMAD calculated by plotting cumulative mass of powder collected at each stage (probability axis) against the effective cutoff diameter (log axis)..

About 3×10^5 A549 cells were exposed to ~6 ng plasmid/well bearing a GFP-IFNγ construct under the CMV promoter, or to particles containing equivalent amount of plasmid. Fluorescence microscopy at different time intervals after exposure of cells to particles revealed that expression of GFP could be observed starting 6h after exposure to particles. At 24h post transfection, GFP co-

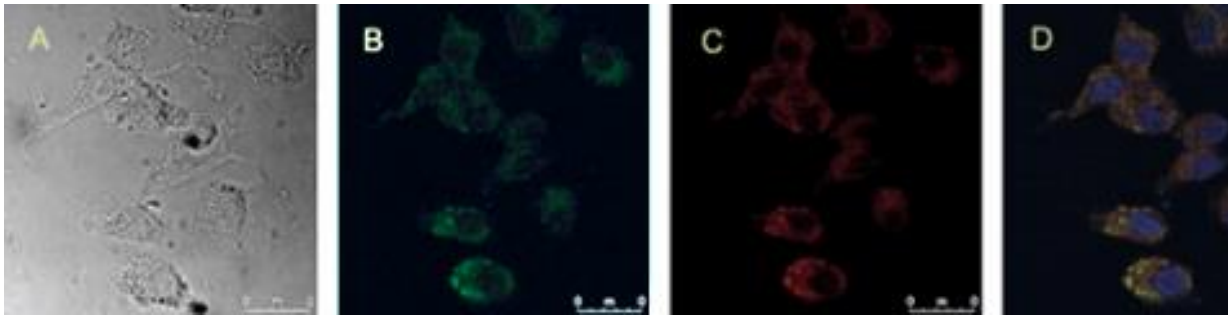

Figure 3: Fluorescence microscopy shows co-localization of GFP-IFN-γ chimeric protein with lysosomes at 24h post-transfection. (A) bright field (B) GFP (C) Lysotracker red (D) Merged image

localized with Lysotracker®, suggesting that the expressed protein was targeted for degradation at this time Lung epithelial cells exposed to DPI particles showed transient expression of green fluorescent protein (GFP) expressed in tandem with IFN-γ from 6-24 h, after which the protein was observed to co-localize with lysosomes (Figure 4).

Mice receiving inhalations of ~100µg of particles containing ~5ng of plasmid DNA with RFP under the CMV promoter were imaged at 6, 12, 24, 36 and 48h post inhalation (Figure A and 5). Control mice received particles comprising all components except DNA. These animals showed background signal in the excretory organs, indicating that dietary components/metabolites/microflora etc. contribute to the fluorescence signals observed. At 12h post dose, mice were also imaged from the ventral aspect. Signal was observed in the nasal/buccal area at this time but other time-points. It is likely that the buccal/nasal mucosal epithelium was also transiently transfected during administration of the inhalation. A preliminary assessment of the kinetics of foreign gene expression was thus arrived at by imaging, suggesting that RFP expression was detectable from 6h onward, peaking at 24h and depleting substantially by 36 and 48h after dosing. These results are summarized in Figure 5.

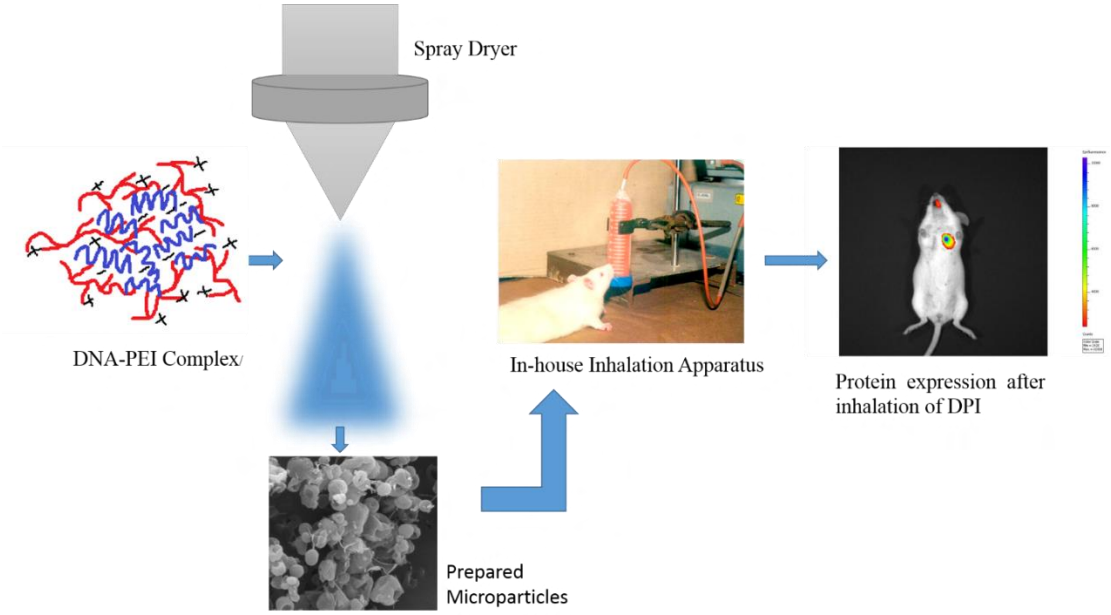

Figure A. Schematic representation depicting the method of preparation and administering the DPI to mice.

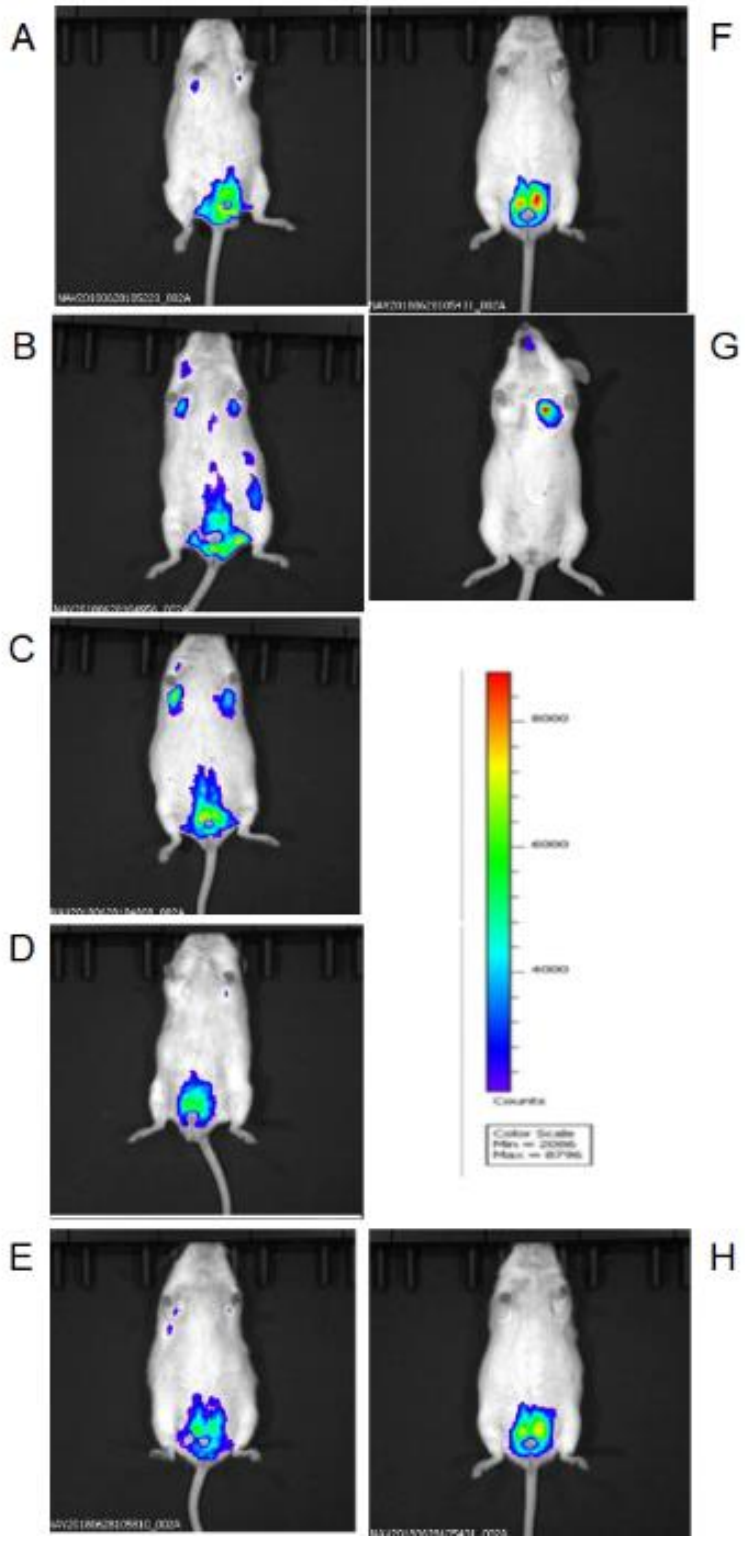

Figure 4: In- vivo imaging of mice at different time intervals after inhalation of plasmid bearing RFP under CMV promoter. (A-E): 6h; 12h, 18h, 24h after inhalation. (F): Animal that received control particles without DNA at 6h. (G): One animal showed signal only in the left lung at 12 h (corresponding to Panel C). (H): Control animal at 48h.

Mice administered the plasmid bearing the IFNγ gene were subjected to bronchioalveolar lavage (BAL) at time-points indicated and ELISA carried out on the BAL fluid to estimate the kinetics of secretion of the functional protein in the lumen of the airways and lungs. Results shown in Figure 6 indicate that secretion of IFN-γ towards the luminal side of the airways and lungs was discernible after 12-24h after inhalation and peaked at 33h. A maximal concentration in the BAL fluid (C_{max}) of about 800 pg/ml was achieved. This value appears comparable to C_{max} values of *ca* 300-1500 Units/ml estimated by radioimmunnoassay in the BAL fluid of human volunteers receiving 250 and 1000µg of the protein by nebulization. Because Jaffe et al administered the protein itself by nebulization, the t_{max} reported by them was obviously the first time-point of sampling (1h). Integrating the curve shown in Figure 6 with respect to time yielded an AUC_{0-48} of 1103 pg/ml×h.

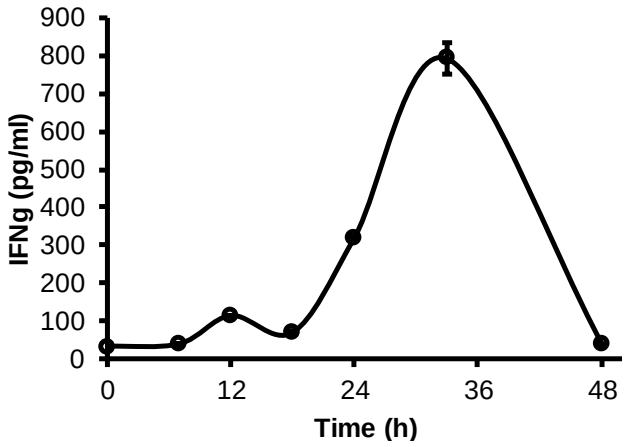

Figure 5: IFN-γ kinetics in BALF of mice administered inhalations. Mean ±SD values (N=3) are plotted.

Lung sections of infected mice receiving a single inhaled dose providing the time kinetics of IFN-γ expression shown above were stained for markers of autophagy. Figure 7 shows that LC3-II and LAMP-1 expression was low in mice that received no treatment, and in treated animals examined 7h after inhalation. After 18h, expression of these markers increased discernibly. The two markers co-localized at 48h post inhalation. Autophagic flux is associated with tissue remodeling as well as with killing of intracellular pathogen.

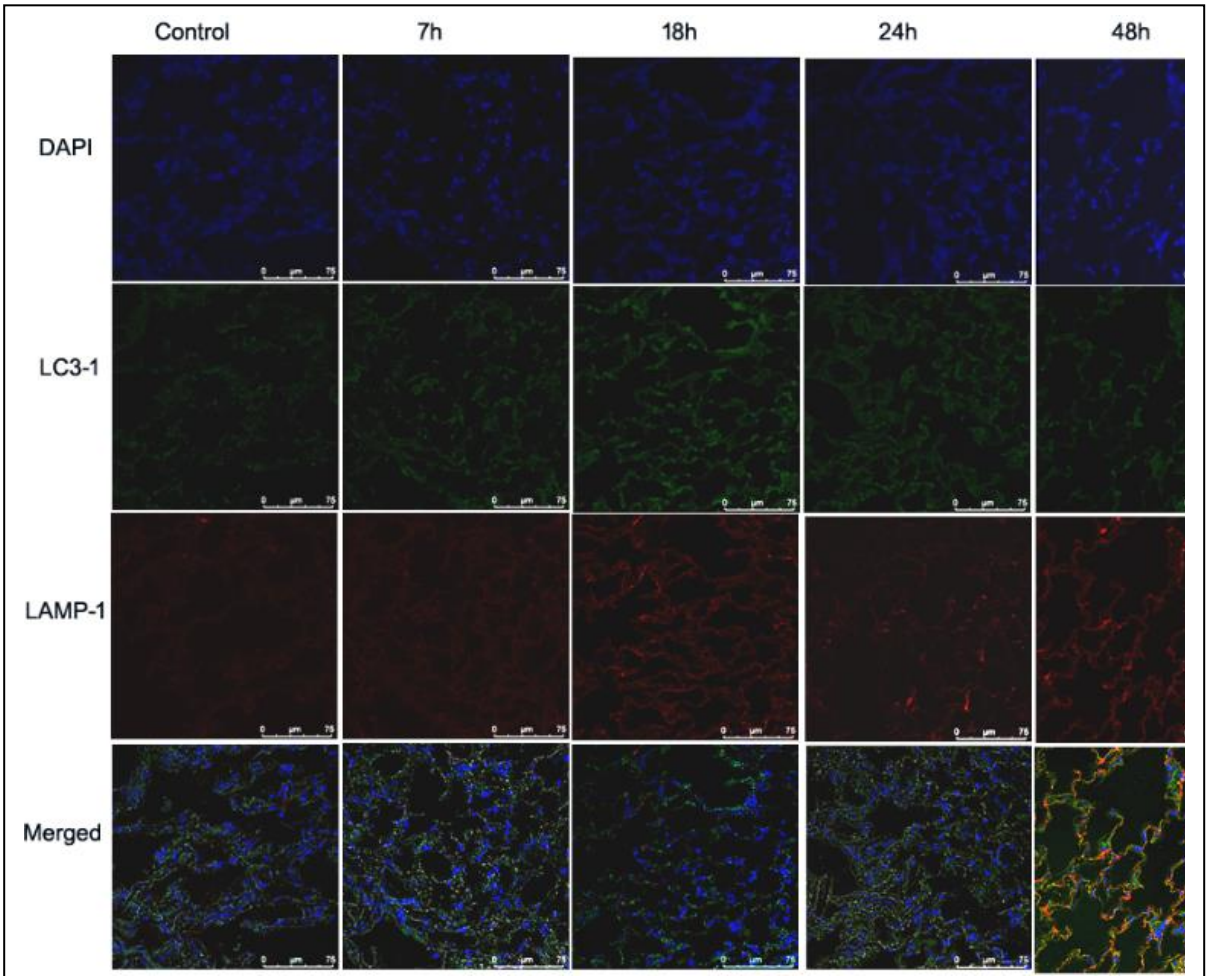

Figure 6: Representative lung sections of mice infected with Mtb 21 days before dosing with inhalations of the plasmid bearing the IFN-γgene indicate progressive induction of autophagy as surrogate pharmacodynamic response to transient transfection of the lung. The response was observed to initiate at 18h and was maximal at the last time-point studied.

Preclinical Efficacy of DPI alone vs DPI as adjunct to DOTS

We infected mice by exposure to a low-dose aerosol of MTB and started treatment 28 days later. By nose-only exposure, the mice were given about 100 µg of the DPI containing about 5 ng of plasmid bearing the mouse gene for IFN-γ (Ifng) with or without concurrent oral treatment with standard

animal-equivalent doses of isoniazid (H), rifampicin (R), pyrazinamide (Z) and ethambutol (E) used for drug-sensitive MTB in the Directly Observed Treatment Short Course (DOTS). Table 3.3 shows the results of a four-week study of five different regimens.

Table 3. 1: Treatment groups and regimens.

Group	Intervention	Frequency and duration	Daily Dose
1.	(No Rx) Untreated control at the start of treatment (28days post-infection)	_	_
2.	(No Rx) Untreated control at the end of treatment (57 days post-infection)	_	_
3.	DOTS	Once a day, five days a week by gavage	HRZE (10,15,35,20 mg/kg)
4.	DOTS + 12 DPI	Once a day, five days a week by gavage and three times a week on alternate days via DPI	HRZE (10,15,35,20 mg/kg) and ~5ng Ifng via DPI
5.	DOTS + 4 DPI	Once a day, five days a week by gavage and once a week via DPI	HRZE (10,15,35,20 mg/kg) and ~5ng Ifng via DPI
6.	12 DPI	Three times a week on alternate days via DPI	and ~5ng Ifng via DPI
7	4 DPI	Once a week via DPI	and ~5ng Ifng via DPI

The mice received an initial inoculum of bacteria amounting to 100 (2-log) colony forming units (CFU) per gram of lung tissue. After 28 days, the infection increased to 6.93±0.29 log CFU/g. Treatment was

started after 28 days, with the animals receiving group-specific regimens as specified in Table 3.3. Following a three-day drug washout period at the end of treatment, the bacterial load in the lungs and spleen of the animals in the treatment and control groups were estimated. The results are depicted graphically in Figure 3.18 and may be summarized as follows.

At the time of final sacrifice, the CFU/g in the untreated controls were 6.22 ± 0.23-log in the lungs and 4.50±0.11-log in the spleen. The bacterial load was decreased by 2.24-log in the lungs and 1.73-log in the spleen after four weeks of treatment with human-equivalent dosages of DOTS medicines. Addition of 12 doses of the DPI led to more significant reduction in the bacterial burden by 2.54-log and 2.66-log in the lungs and spleen respectively. Importantly, adding four DPI doses to DOTS drug decreased lung bacterial load by 2.96-log, which was higher than the reduction produced by adding 12 doses to DOTS drugs. The DOTS+4 DPI group and the untreated control (No Rx) groups each had one mouse die before the conclusion of the treatment period, therefore they were removed from the analysis. In animals given four doses of the DPI in addition to DOTS, the spleen load was decreased by 1.52-log. At the end of four weeks, the majority of animals given DOTS medicines, with or without the DPI, had no culturable bacteria in their spleen. In groups receiving DOTS with or without concurrent DPI dosages, there was no statistically significant change in lung or spleen load. If DOTS medicines were withdrawn, there was no significant difference in lung or spleen load between untreated controls and those that received either of the two DPI regimens as a stand-alone intervention.

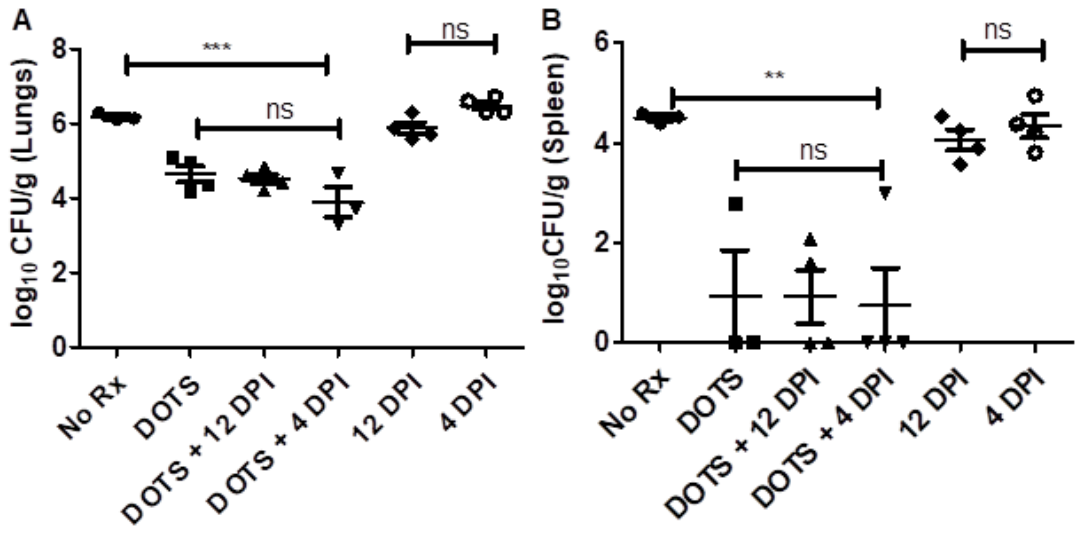

Figure 8.Bacterial burden (CFU/g) in MTB-infected lungs (A) and spleen (B) of mice in different groups (N= 3 or 4/group). Scatter points indicate values from individual animals. The arithmetic mean is indicated by a horizontal line. Error bars show standard deviations. Statistical significance of differences was calculated by ANOVA followed by means comparison using Tukey's test. One, two and three asterisks (*) represent P<0.01, 0.001 and 0.0001; 'ns' indicates 'not significant' at P<0.01.

These results suggest that over the course of four weeks, four or 12 doses of a DPI containing 5ng plasmid DNA capable of transfecting the respiratory epithelium of MTB-infected mice to create IFN-γ *in situ* can only lower the bacterial load in the lungs and spleen minimally. The CFU/g decrease is not statistically significant. These findings were predicted. IFN-γ may have a role in the pathogenesis of tuberculosis, however if infection is well-established on a wide scale, it is unlikely to generate cellular or molecular microbicidal effector activities in macrophages or lymphocytes. Although a potential tuberculosis vaccine administered to 1399 children resulted in a net increase in the number of T cells that generate IFN-γ, vaccination effectiveness did not improve in tandem. Similarly, it has been pointed out that introducing IFN-γ as a bactericidal intervention for salvage therapy doesn't really benefit TB patients with advanced illness. Bacteria can grow in large numbers in extracellular necrotizing tuberculosis. Extracellular MTB is prone to generate biofilms that are resistant to host defense mechanisms.Multiple signaling molecules, including Type I and Type II

interferons, GM-CSF (granulocyte-macrophage colony stimulating factor), TNF (tumor necrosis factor), chemokines induced by Interleukin (IL)-17 and IL-23, and T cell effector functions that are not dependent on IFN-γ, all play a role in controlling MTB proliferation and granuloma formation in the lungs.

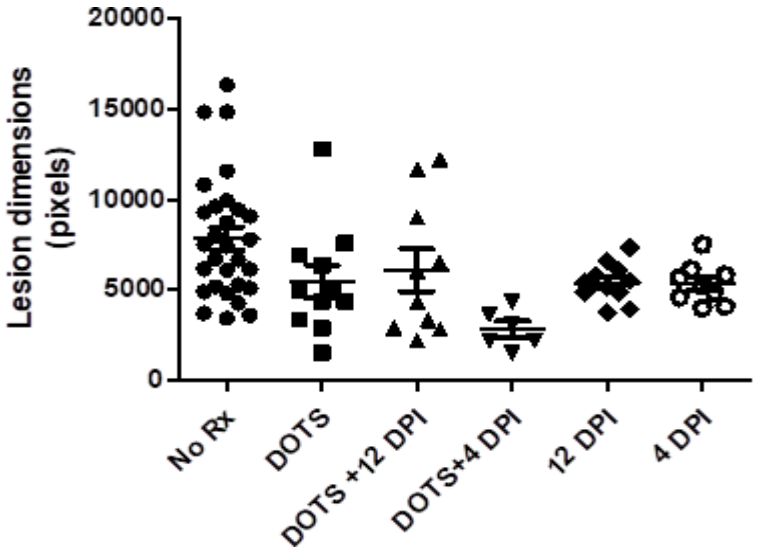

Figure 9.Morphometry. Nodular lesions visible in the photographs of lungs collected at terminal sacrifice. Scatter points represent individual lesions, means are shown by a horizontal line and error bars represent standard error of mean. The only statistically significant difference in ANOVA followed by Bonferroni's test for means comparison at the level of 0.05 was observed in respect of the group receiving DOTS+ 4 doses of the DPI (t Value= -3.3, probability = 0.018).

Transient gene therapy with IFN-γ, without concomitant use of first-line anti-TB drugs as antitubercular chemotherapy, was not sufficient to significantly and consistently kill TB bacteria in the lungs or spleen .However, it elicited molecular and cellular responses that resolved nodular lesions in the lungs and partially restored alveolar architecture. In general terms, stand-alone HDT was not efficient in eliciting significant bactericidal host responses that could 'kill the bug' but the functional protein elicited such responses that could 'heal the host.' If these observations are borne out in human patients, this effect is likely to be clinically useful. It is submitted that the prototype product is ready for detailed preclinical investigation of safety and efficacy. Such studies should not address intended use as "salvage" therapy for patients with multibacillary advanced disease. Instead, it should be investigated as "adjunct" therapy in individuals who might benefit from it in terms of preventing severe immunopathology.